Journal of Solid Mechanics Vol. 10, No. 4 (2018) pp. 702-718

Quasi-Static Deformation of a Uniform Thermoelastic Half –Space Due to Seismic Sources and Heat Source

A.K. Vashishth [1,*], K. Rani [2]

[1]*Department of Mathematics, Kurukshetra University, Kurukshetra 136119, India*
[2]*Department of Mathematics, CMG Govt. College for Women, Bhodia Khera, Fatehabad 125050, India*

Received 1 July 2018; accepted 2 September 2018

ABSTRACT

This paper investigates the quasi-static plane deformation of an isotropic thermoelastic half-space due to buried seismic sources and heat source. Governing equations of thermo-elasticity are solved to obtain solutions for seismic sources in a thermoelastic half-space. The general solutions are acquired with the aid of Laplace and Fourier transforms and with the use of boundary conditions. The case of dip-slip line dislocation is studied in detail along with line heat source. Analytical solutions for two limiting cases: adiabatic and isothermal, are obtained. The solutions for displacement, stresses and temperature in space-time domain are obtained by using a numerical inversion procedure. The accuracy of the proposed method is verified through a comparison of the results obtained with the existing solutions for elastic medium. In addition, numerical results for displacements, stresses and temperature function, induced by a vertical dip-slip dislocation and line heat source, are presented graphically to illustrate the effect of inclusion of thermal effect in simulation of the problem.

Keywords : Thermoelastic; Seismic source; Dip-slip dislocation; Plane deformation; Heat source.

1 INTRODUCTION

THE study of the Earth deformation, associated with faults due to earthquakes, has been a subject of great interest for geophysicists and seismologists. To investigate the deformation associated with faults, the Earth is often modelled as an elastic half-space [1-19]. Two dimensional dip-slip dislocation models of earthquake faults have been used extensively by many researchers. Based on the pioneer work of Singh and Garg [20] on two dimensional seismic sources, several articles [21-32] on deformation caused by dip-slip line dislocation sources have been appeared in literatures. In most of these studies, the medium has been considered as a uniform elastic half-space or two half-spaces in a welded contact or a layer over an elastic half-space containing seismic sources.

As the temperature inside the Earth is not constant and it plays a significant role in geophysical studies, so it becomes more appropriate to consider thermoelastic model of the Earth rather than the elastic one. Some researchers have modelled the Earth as a thermoelastic medium and studied the deformation due to thermal and mechanical

*Corresponding author.
E-mail address: akvashishth@kuk.ac.in (A.K. Vashishth).

sources. Pan [33] studied the transient thermoelastic deformation in a transversely isotropic and layered half-space by surface loads and internal sources. The thermoelastic coupling was neglected in the heat equation. The expressions for thermoelastic displacements and stresses in a multi-layered elastic media due to varying temperature and concentrated point loads were determined by Ghosh and Kanoria [34]. Hou et al. [35] derived Green's functions for a line heat source in a semi-infinite thermoelastic plane. Jacquey et al. [36] studied thermoelastic effects on fault slip tendency during injection and production of geothermal fluids. Marin et al. [37] discussed reciprocity theorem in micro-stretch thermoelastic bodies. Vashisth et al. [38] studied the deformation of a thermoelastic medium due to seismic source in a welded contact elastic medium. Naeeni and coauthors [39-43] studied dynamic problems of transient response of a thermoelastic half-space subjected to mechanical and thermal buried sources. Kordkheili et al. [44] made an axisymmetric analysis of a thermoelastic isotropic half-space under buried mechanical loads and heat flux to determine the displacement and temperature functions. Nowacki [45] made an attempt to find solution for a three dimensional quasi-static problem in thermo-elasticity and obtained solution for point source and centre of compression. The quasi-static deformation of a semi-infinite thermoelastic medium caused by two or three dimensional seismic sources (strike-slip fault, dip-slip fault and centre of rotation etc.) has not been studied so far.

The quasi-static deformation of a homogeneous isotropic thermoelastic half-space due to two dimensional buried seismic sources and line heat source is considered in the present study. The expressions for temperature function, stresses and displacements have been obtained in Laplace transform domain using Airy stress function approach and traction free boundary conditions. The case of dip-slip line dislocation source is studied in detail and the solutions are obtained analytically for two limiting cases: adiabatic and isothermal. The solutions in space time domain are computed numerically for a dip-slip fault and line heat source and are presented graphically. The work of Rani et al. [9] and Hou et al. [35] has been obtained as a particular case of this study. The theoretical expressions of solutions for different seismic sources given by Rani and Singh [22] again based upon the solutions given by [9] for elastic half-space, have been used in a number of observational seismological studies [46-52]. Such fundamental solutions have not been derived for a thermoelastic medium so far.

This work is motivated by the fact that in the interior of the Earth, deep focus earthquakes occur and temperature plays a significant role there. The mechanism for deep focus earthquakes depends strongly on the thermal structure of the Earth [53]. The critical difference between the present and earlier studies is that there is a noticeable change in the temperature function in the presence of seismic source. In the light of these findings, it can be concluded that the thermal effect should be included in calculating the deformation in order to obtain more realistic studies of earthquakes. Thus, modelling the Earth as a thermoelastic medium is appropriate and is an advancement in the existing models.

2 FORMULATION OF THE PROBLEM

Consider a homogeneous isotropic thermoelastic half space $(z \geq 0)$. Let us represent Lame's constants by λ, μ; the thermoelastic coupling coefficient by β; the coefficient of linear thermal expansion by α_t; Poisson's ratio by υ; the thermal conductivity by λ_0; the specific heat by C_e; the density by ρ and the temperature at natural state by T_0. A line source parallel to the *x*-axis passing through the point $(0,0,h)$ in the thermoelastic half space is considered (Fig. 1).

A two dimensional plane strain problem in *yz*-plane is considered so that the displacement components can be written as:

$$u_i = u_i(y,z,t),\ u_x = 0 \text{ for all } i = y,z. \tag{1}$$

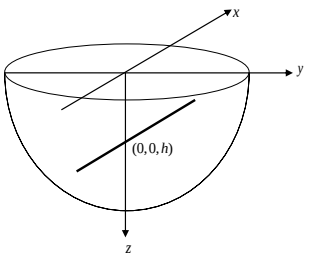

Fig.1
A line source acting through the point $(0,0,h)$.

3 BASIC EQUATIONS AND THEIR SOLUTIONS

The equations of equilibrium and heat equation, in case of plane strain problem, are

$$(\lambda+\mu)u_{i,ij}+\mu\nabla^2 u_j-\beta\theta_{,j}+f_j=0 \tag{2}$$

$$\lambda_0\nabla^2\theta-\rho C_e\dot{\theta}-\beta T_0\dot{u}_{j,j}+Q=0\ ,\ (i,j=y,z) \tag{3}$$

where, θ is the difference between current and the reference temperature, f_j are components of body force, Q is the heat source term and ∇^2 is the Laplacian operator. For a line force, $f_j=F_j\delta(y)\delta(z-h)H(t)$, $Q=0$ and for line heat source $f_j=0$, $Q=q'\delta(y)\delta(z-h)H(t)$. Here F_y and F_z are horizontal and vertical forces per unit length respectively and q' is the heat generated per unit length. $\delta(.)$ is the Dirac delta function and $H(.)$ is the Heaviside unit step function.

Following Banerjee [54], the fundamental solutions (displacements and temperature difference function) for a single line force (horizontal and vertical) and line heat source applied in a thermoelastic medium are obtained first. Secondly, the solutions for dipolar sources are obtained by following the procedure as given in [55].

If $u_i^{(j)}$ is the ith component of the displacement due to force in jth direction, then $u_i^{(jk)}=-u_{i,k}^{(j)}$, $(i,j,k=y,z)$ represents, for $j\neq k$, displacement for a horizontal single couple (jk) in yz plane with force along jth direction and offset along kth direction. For dipole, $j=k$.

The results for double couple can be obtained by adding or subtracting the corresponding results of single couples or dipoles e.g. $(yz)+(zy)$ is a double couple that corresponds to a vertical dip-slip line dislocation and $(zz)-(yy)$ is a double couple which corresponds to a dip-slip on a 45° dipping dislocation [3].

A plane deformation problem in an isotropic thermoelastic medium can be solved in terms of the Airy stress function U and temperature difference function θ [56]. The Airy stress function U is defined as:

$$\sigma_{yy}=\frac{\partial^2 U}{\partial z^2},\ \sigma_{zz}=\frac{\partial^2 U}{\partial y^2},\ \sigma_{yz}=-\frac{\partial^2 U}{\partial y\,\partial z} \tag{4a}$$

where σ_{ij} are components of stress tensor and are related to displacements as:

$$\sigma_{ij}=(\lambda u_{k,k}-\beta\theta)\delta_{ij}+\mu(u_{i,j}+u_{j,i}) \tag{4b}$$

and δ_{ij} is Kronecker delta.

Neglecting body force and heat source terms in Eqs. (2)-(3) and applying Laplace transform with respect to time t on Eqs. (2)-(4) and simplifying further (see Appendix A), we obtain

$$\nabla^2(\nabla^2\bar{U}+2\eta\bar{\theta})=0 \tag{5}$$

$$\lambda_0\nabla^2\bar{\theta}-s\left(\rho C_e+\frac{\alpha_0{}^2T_0}{\mu(1-2\upsilon)}\right)\bar{\theta}-\frac{s\alpha_0T_0}{2\mu}(\nabla^2\bar{U})=0 \tag{6}$$

where s is the variable of Laplace transform, $\bar{U}$ and $\bar{\theta}$ are functions of y, z and s. The notation bar over a variable denotes the Laplace transform of that variable. Hereafter, this notation is suppressed for brevity.

Elimination of θ and U, one at a time, from Eqs. (5)-(6) gives

$$(c\nabla^2-s)\nabla^2\theta=0\ ,\ (c\nabla^2-s)\nabla^4U=0 \tag{7}$$

where $c=\dfrac{\lambda_0\left(\lambda+2\mu\right)}{\rho C_e\left(\lambda_s+2\mu\right)}$, $\lambda_s=\lambda+\dfrac{T_0\beta^2}{\rho C_e}$.

To solve Eq. (7), first Fourier Sine/ Cosine transform with respect to y is taken, the resulting differential equations are solved and then θ and U are obtained by taking inverse Fourier Sine/ Cosine transforms respectively. Such a solution for a line source, parallel to the x-axis and passing through the point $(0,0,h)$ in an unbounded thermoelastic medium, can be written as:

$$U_0=\int_0^\infty\left(L_0e^{-m|z-h|}+(M_0+N_0k\,|z-h|)e^{-k|z-h|}\right)\begin{pmatrix}\sin ky\\ \cos ky\end{pmatrix}dk \tag{8}$$

$$\theta_0=\int_0^\infty\left(\frac{s}{\gamma_1}\zeta L_0e^{-m|z-h|}+N_0k^2\zeta e^{-k|z-h|}\right)\begin{pmatrix}\sin ky\\ \cos ky\end{pmatrix}dk \tag{9}$$

where $m=\left(k^2+\dfrac{s}{c}\right)^{1/2}$, $\gamma_1=-2\eta c\zeta$, $\zeta=\dfrac{2(\upsilon_s-\upsilon)}{\alpha_0}$, $\upsilon_s=\dfrac{\lambda_s}{2\left(\lambda_s+\mu\right)}$.

The expression $I=\begin{pmatrix}\sin ky\\ \cos ky\end{pmatrix}$ represents a linear combination of $\sin ky$ and $\cos ky$. Only one term, either the upper term or the lower term, is to be selected.

Using the expressions of displacements and temperature function of [54], the stresses were obtained and Laplace transform was taken thereafter. Making use of tables of integral transform [57], the expressions of stresses and temperature, in integral form, were obtained. These expressions and the expressions obtained from Eqs. (8) and (9) are compared to obtain the source coefficients L_0, M_0 and N_0 for different line sources and dipolar sources. L_0, M_0 and N_0 are obtained as:

Horizontal line force:

$$L_0=\frac{cc_1kF_y}{2\pi(1-\upsilon)s^2m},\ M_0=-\frac{F_y}{4\pi s(1-\upsilon)k^2}\left(1-2\upsilon-c_1+\frac{2cc_1k^2}{s}\right),\ N_0=\frac{(1+c_1)F_y}{4\pi(1-\upsilon)sk^2},\ c_1=\frac{\upsilon_s-\upsilon}{1-\upsilon_s} \tag{10}$$

with the stipulation that in the representation of integrals , the upper term of $I=\begin{pmatrix}\sin ky\\ \cos ky\end{pmatrix}$ is to be selected.

Vertical line force:

$$L_0=\pm\frac{cc_1F_z}{2\pi(1-\upsilon)s^2},\ M_0=\pm\left(\frac{F_z}{2\pi sk^2}-\frac{F_zcc_1}{s^22\pi(1-\upsilon)}\right),\ N_0=\pm\frac{(1+c_1)F_z}{4\pi(1-\upsilon)sk^2} \tag{11}$$

with the stipulation of selecting lower term of I. The upper and lower sign of $\pm$ corresponds to the region $z>h$ and $z<h$ respectively.

Line heat source:

$$L_0=-\frac{\beta c\,\mu q'}{\pi m\,\lambda_0(\lambda+2\mu)s^2},\ M_0=\frac{\beta c\,\mu q'}{\pi k\,\lambda_0(\lambda+2\mu)s^2},\ N_0=0 \tag{12}$$

with the stipulation of selecting the corresponding lower term of I.

Double couple $(yz)+(zy)$:

$$L_0=\pm\frac{cc_1kD_{yz}}{\pi(1-\upsilon)s^2},\ M_0=\mp\frac{cc_1kD_{yz}}{\pi(1-\upsilon)s^2},\ N_0=\pm\frac{(1+c_1)D_{yz}}{2\pi(1-\upsilon)sk},\ D_{yz}=\mu b\,dl \tag{13}$$

where D_{yz} is the moment of the double couple, b is the slip and dl is the width of the dislocation. Here, upper term of I is selected.

Double couple $(zz)-(yy)$:

$$L_0=\frac{c_1c\left(m^2+k^2\right)D'_{yz}}{2\pi\left(1-\upsilon\right)ms^2},\ M_0=-\frac{c_1ckD'_{yz}}{\pi\left(1-\upsilon\right)s^2},\ N_0=\frac{\left(1+c_1\right)D'_{yz}}{2\pi\left(1-\upsilon\right)sk},\ D'_{yz}=\mu b\,dl \tag{14}$$

with the stipulation of selecting lower term of I.

Thus, the expressions for temperature difference function and Airy stress function for the whole half-space become

$$U=U_0+\int_0^\infty(Le^{-mz}+(M+Nkz)e^{-kz})\begin{pmatrix}\sin ky\\ \cos ky\end{pmatrix}dk \tag{15}$$

$$\theta=\theta_0+\zeta\int_0^\infty(\frac{s}{\gamma_1}Le^{-mz}+k^2Ne^{-kz})\begin{pmatrix}\sin ky\\ \cos ky\end{pmatrix}dk \tag{16}$$

where L, M and N are arbitrary constants and may be functions of k and can be obtained by using boundary conditions. U_0 and θ_0 are given in Eqs. (8) and (9).

Eqs. (4a), (10)-(16) give

$$\sigma_{yy}=\int_0^\infty[m^2L_0e^{-m|z-h|}+k^2(M_0-2N_0+N_0k\left|z-h\right|)e^{-k|z-h|}+m^2Le^{-mz}+k^2(M-2N+Nkz)e^{-kz}]\begin{pmatrix}\sin ky\\ \cos ky\end{pmatrix}dk \tag{17}$$

$$\sigma_{yz}=\int_0^\infty[\pm(mL_0e^{-m|z-h|}+k\left(M_0-N_0(1-k\left|z-h\right|)\right)e^{-k|z-h|})+mLe^{-mz}+k\left(M-N\left(1-kz\right)\right)e^{-kz}]k\begin{pmatrix}\cos ky\\ -\sin ky\end{pmatrix}dk \tag{18}$$

$$\sigma_{zz}=\int_0^\infty[L_0e^{-m|z-h|}+(M_0+N_0k\left|z-h\right|)e^{-k|z-h|}+Le^{-mz}+(M+Nkz)e^{-kz}]\begin{pmatrix}\sin ky\\ \cos ky\end{pmatrix}\left(-k^2\right)dk \tag{19}$$

The displacement components can now be written as:

$$2\mu u_y=-\int_0^\infty\left[L_0e^{-m|z-h|}+(M_0+N_0(2\upsilon_s-2+k\left|z-h\right|))e^{-k|z-h|}+Le^{-mz}+(M+N\left(2\upsilon_s-2+kz\right))e^{-kz}\right]k\begin{pmatrix}\cos ky\\ -\sin ky\end{pmatrix}dk \tag{20}$$

$$2\mu u_z=\int_0^\infty\left[\pm(mL_0e^{-m|z-h|}+(M_0+N_0(1-2\upsilon_s+k\left|z-h\right|))ke^{-k|z-h|})+mLe^{-mz}+(M+N\left(1-2\upsilon_s+kz\right))ke^{-kz}\right]\begin{pmatrix}\sin ky\\ \cos ky\end{pmatrix}dk \tag{21}$$

The normal heat flux is obtained as:

$$q_z=-\lambda_0\theta_{,z}=\lambda_0\zeta\int_0^\infty\left[\pm\left(\frac{s}{\gamma_1}mL_0e^{-m|z-h|}+k^3N_0e^{-k|z-h|}\right)+\frac{s}{\gamma_1}mLe^{-mz}+k^3Ne^{-kz}\right]\begin{pmatrix}\sin ky\\ \cos ky\end{pmatrix}dk \tag{22}$$

4 BOUNDARY CONDITIONS

The surface $z=0$ is traction free, so the boundary conditions are

$$\sigma_{yz} = 0, \ \sigma_{zz} = 0 \quad \text{at} \quad z = 0 \tag{23}$$

Further, if there is no flow of heat at the free surface, then

$$q_z = 0 \quad \text{at} \quad z = 0 \tag{24a}$$

or if the temperature remains constant across the boundary, then

$$\theta = 0 \ \text{at} \ z = 0 \tag{24b}$$

Let $L_0^+\left(L_0^-\right)$, $M_0^+\left(M_0^-\right)$ and $N_0^+\left(N_0^-\right)$ represent source coefficients according to $z > h\left(z < h\right)$. The boundary conditions (23) and (24a) yield the system

$$\begin{aligned} &mL + kM - kN = mL_0^- e^{-mh} + (M_0^- + N_0^- kh - N_0^-)ke^{-kh} \\ &L + M = -L_0^- e^{-mh} - (M_0^- + N_0^- kh)e^{-kh} \\ &\frac{ms}{\gamma_1} L + k^3 N = \frac{ms}{\gamma_1} L_0^- e^{-mh} + k^3 N_0^- e^{-kh} \end{aligned} \tag{25a}$$

On solving these equations, we get

$$\begin{aligned} L &= \left(1+\delta_1\right) L_0^- e^{-mh} + \delta_1 \left(M_0^- + N_0^- kh\right) e^{-kh} \\ M &= \left(-2-\delta_1\right) L_0^- e^{-mh} + \left(-1-\delta_1\right)\left(M_0^- + N_0^- kh\right) e^{-kh} \\ N &= \frac{-2}{\left(1+\Omega\right)}\left[L_0^- e^{-mh} + \left(M_0^- + N_0^- kh\right) e^{-kh}\right] + N_0^- e^{-kh} \end{aligned} \tag{25b}$$

where $\delta_1 = \dfrac{2\Omega k}{\left(m-k\right)\left(1+\Omega\right)}$, $\Omega = \dfrac{k^2 \gamma}{m(m+k)}$, $\gamma = \dfrac{2(\upsilon - \upsilon_s)}{1-\upsilon}$.

Similarly, the boundary conditions (23) and (24b) yield the system

$$\begin{aligned} &mL + kM - kN = mL_0^- e^{-mh} + (M_0^- + N_0^- kh - N_0^-)ke^{-kh} \\ &L + M = -L_0^- e^{-mh} - (M_0^- + N_0^- kh)e^{-kh} \\ &\frac{s}{\gamma_1} L + k^2 N = -\frac{s}{\gamma_1} L_0^- e^{-mh} - k^2 N_0^- e^{-kh} \end{aligned} \tag{26a}$$

On solving these equations, we get

$$\begin{aligned} L &= \left(-1+m\delta_2\right) L_0^- e^{-mh} + k\,\delta_2 \left(M_0^- + N_0^- kh - N_0^-\right) e^{-kh} \\ M &= -m\delta_2 L_0^- e^{-mh} - \left(1+k\,\delta_2\right)\left(M_0^- + N_0^- kh\right) e^{-kh} + k\,\delta_2 N_0^- e^{-kh} \\ N &= \frac{-2}{\left(k+m\Omega\right)}\left[mL_0^- e^{-mh} + k\left(M_0^- + N_0^- kh\right) e^{-kh}\right] + \frac{k-m\Omega}{\left(k+m\Omega\right)} N_0^- e^{-kh} \end{aligned} \tag{26b}$$

where $\delta_2 = \dfrac{2\Omega m}{\left(m-k\right)\left(k+m\Omega\right)}$.

Substituting the values of *L, M, N* from Eqs. (25b) or (26b) in Eqs. (15)-(22), we get the integral expressions for the Airy stress function, temperature difference function, stress components, displacement components and the heat

flux in the thermoelastic half-space in terms of the source coefficients L_0^-, M_0^- and N_0^-. These integrals can be solved numerically. However, analytical solutions can also be found for following two particular cases:

Case (i) $t \to 0$ which further implies that no net flow of heat takes place i.e. the adiabatic condition.

Case (ii) $t \to \infty$ which further implies the isothermal condition for seismic sources and steady state heat conduction for the line heat source.

5 SOLUTIONS FOR A VERTICAL DIP-SLIP DISLOCATION

The solutions, corresponding to a vertical dip-slip dislocation in the half-space having thermally isolated surface, can be obtained by Eqs. (13), (15) -(24a) and (25b). The results, in analytical form for the two limiting cases, are obtained as:

Case (i) Adiabatic case

$$U = \frac{D_{yz}}{2\pi(1-\upsilon_s)}\left[\pm\frac{y\,|z-h|}{R_1^2} - \frac{y\,(z-h)}{R_2^2} + \frac{4hyz\,(h+z)}{R_2^4}\right] \tag{27}$$

$$\sigma_{yy} = \frac{D_{yz}\,y}{2\pi(1-\upsilon_s)}\left[\pm\left(-6+8\frac{(z-h)^2}{R_1^2}\right)\frac{|z-h|}{R_1^4} + \frac{2(5h+3z)}{R_2^4} - 8(h+z)(z^2+3h^2+10hz)\frac{1}{R_2^6} + 96hz\,\frac{(h+z)^3}{R_2^8}\right] \tag{28}$$

$$\sigma_{zz} = \frac{D_{yz}\,y}{2\pi(1-\upsilon_s)}\left[\frac{2(z-h)}{R_1^4}\left(1-\frac{4|z-h|^2}{R_1^2}\right) - \left(\frac{2(z-h)}{R_2^4} - \frac{8(z^2-h^2+6hz)(h+z)}{R_2^6} + \frac{96hz\,(h+z)^3}{R_2^8}\right)\right] \tag{29}$$

$$\begin{aligned}\sigma_{yz} = \frac{-D_{yz}}{2\pi(1-\upsilon_s)}\Bigg[&-\frac{1}{R_1^2} + \frac{1}{R_2^2} + \frac{8|z-h|^2}{R_1^4} - \frac{8|z-h|^4}{R_1^6} - \frac{8(z+h)^2+12hz}{R_2^4} \\ &+ \frac{8((z+h)^2+12hz)(h+z)^2}{R_2^6} - \frac{96hz\,(h+z)^4}{R_2^8}\Bigg]\end{aligned} \tag{30}$$

$$\begin{aligned}2\mu u_y = \frac{D_{yz}}{2\pi(1-\upsilon_s)}\Bigg[&\frac{z-h}{R_1^2}\left(3-2\upsilon_s-2\frac{|z-h|^2}{R_1^2}\right) + \frac{h-z-2(1-\upsilon_s)(z+3h)}{R_2^2} \\ &+ \frac{2(z+h)\big((z+h)(z-h+4(1-\upsilon_s)h)+6hz\big)}{R_2^4} - \frac{16hz\,(z+h)^3}{R_2^6}\Bigg]\end{aligned} \tag{31}$$

$$\begin{aligned}2\mu u_z = \frac{D_{yz}\,y}{2\pi(1-\upsilon_s)}\Bigg[&\frac{1}{R_1^2}\left((1-2\upsilon_s)+\frac{2|z-h|^2}{R_1^2}\right) \\ &-\frac{1}{R_2^2}\left((1-2\upsilon_s)+\frac{2\big((z+h)(z-h-2h(1-2\upsilon_s))+2hz\big)}{R_2^2} - \frac{16hz\,(z+h)^2}{R_2^4}\right)\Bigg]\end{aligned} \tag{32}$$

$$\theta = \frac{\zeta D_{yz}\,y}{\pi(1-\upsilon_s)}\left[\frac{(z-h)}{R_1^4} - \frac{(z+3h)}{R_2^4} + \frac{8h(h+z)^2}{R_2^6}\right] \tag{33}$$

where $R_1^2 = y^2+(z-h)^2$ and $R_2^2 = y^2+(z+h)^2$.

Case (ii) Isothermal case

The expressions for Airy stress function, stress components and displacement components for the isothermal case can be obtained from those of Case (i) when we replace υ_s by υ. Here, $\theta \to 0$. These reduced results coincide with the corresponding results for a source in an isotropic uniform elastic half-space [9] with some corrections.

6 DIP-SLIP ON A 45° DIPPING DISLOCATION

Using Eqs. (14)-(24a) and (25b), the closed form solutions are obtained as:

Case (i) Adiabatic case

$$U = \frac{D'_{yz}}{2\pi(1-\upsilon_s)}\left[\frac{|z-h|^2}{R_1^2}+\frac{(z+h)(z-h)+2hz}{R_2^2}-\frac{4hz\,(h+z)^2}{R_2^4}\right] \tag{34}$$

$$\sigma_{yy} = \frac{D'_{yz}}{2\pi(1-\upsilon_s)}\left[\frac{2}{R_1^2}+\frac{2}{R_2^2}-\frac{10|z-h|^2}{R_1^4}+\frac{8|z-h|^4}{R_1^6}-\frac{4(z+h)^2+6(z+h)(z+3h)+12hz}{R_2^4} + \frac{8((z+h)(z+3h)+12hz)(h+z)^2}{R_2^6}-\frac{96hz\,(z+h)^4}{R_2^8}\right] \tag{35}$$

$$\sigma_{zz} = \frac{D'_{yz}}{2\pi(1-\upsilon_s)}\left[\frac{2|z-h|^2}{R_1^4}\left(3-\frac{4|z-h|^2}{R_1^2}\right)+\frac{6}{R_2^4}\left(2hz+z^2-h^2\right)-\frac{8(z^2-h^2+12hz)(h+z)^2}{R_2^6}+\frac{96hz\,(h+z)^4}{R_2^8}\right] \tag{36}$$

$$\sigma_{yz} = \frac{D'_{yz}\,y}{2\pi(1-\upsilon_s)}\left[\pm\frac{4|z-h|}{R_1^4}\mp\frac{8|z-h|^3}{R_1^6}+\frac{4(z+h)}{R_2^4}-\frac{8(h+z)((z+h)^2+6hz)}{R_2^6}+\frac{96hz\,(h+z)^3}{R_2^8}\right] \tag{37}$$

$$2\mu u_y = \frac{D'_{yz}\,y}{2\pi(1-\upsilon_s)}\left[(2\upsilon_s-2)\left(\frac{1}{R_1^2}+\frac{1}{R_2^2}\right)+2\frac{|z-h|^2}{R_1^4}+ + \frac{2\left((z+h)(z-h+4(1-\upsilon_s)h)+2hz\right)}{R_2^4}-\frac{16hz\,(z+h)^2}{R_2^6}\right] \tag{38}$$

$$2\mu u_z = \frac{D'_{yz}}{2\pi(1-\upsilon_s)}\left[\pm\left(\frac{(-2\upsilon_s)|z-h|}{R_1^2}+\frac{2|z-h|^3}{R_1^4}\right)+\frac{2(1-\upsilon_s)(z+3h)-2(z+h)}{R_2^2} + \frac{2(z+h)\left((z+h)(z+h-2h(2-2\upsilon_s))+6hz\right)}{R_2^4}-\frac{16hz\,(z+h)^3}{R_2^6}\right] \tag{39}$$

$$\theta = \frac{\zeta D'_{yz}}{2\pi(1-\upsilon_s)}\left[-\frac{1}{R_1^2}-\frac{1}{R_2^2}+\frac{2(z-h)^2}{R_1^4}+\frac{2(z+h)^2+12h(z+h)}{R_2^4}-\frac{16h(h+z)^3}{R_2^6}\right] \tag{40}$$

Case (ii) Isothermal case

As explained earlier, the results for this case can be obtained from the Eqs. (34) -(40) and the reduced results resemble with correct forms of the results of [9].

7 DIP-SLIP DISLOCATION ON AN INCLINED PLANE

The Airy stress function and temperature function due to dip-slip on an inclined plane can be expressed as:

$$U = \mu bdl\left[\frac{\cos 2\delta}{D_{yz}}U^{(yz)+(zy)} + \frac{\sin 2\delta}{D'_{yz}}U^{(zz)-(yy)}\right] \tag{41}$$

$$\theta = \mu bdl\left[\frac{\cos 2\delta}{D_{yz}}\theta^{(yz)+(zy)} + \frac{\sin 2\delta}{D'_{yz}}\theta^{(zz)-(yy)}\right] \tag{42}$$

where δ is the dip angle and $U^{(yz)+(zy)}$, $U^{(zz)-(yy)}$, $\theta^{(yz)+(zy)}$ and $\theta^{(zz)-(yy)}$ can be obtained by using Eqs. (13)-(16) and (25b) for general case and from Eqs. (27), (33), (34) and (40) in particular cases. The displacements and stresses can be obtained similarly.

8 NUMERICAL RESULTS AND DISCUSSION

For the numerical computation of the obtained results, a thermoelastic solid half-space is considered and the parameters are taken from [58-59] and are given in Table 1.

Table 1
Values of parameters of thermoelastic medium.

Thermo-elastic Parameter (Units)	$\mu\left(kg\,m^{-1}s^{-2}\right)$	$\lambda\left(kg\,m^{-1}s^{-2}\right)$	$\alpha_t\left(K^{-1}\right)$	$\rho\left(kg\,m^{-3}\right)$	$T_0(K)$	$C_e(m^2K^{-1}s^{-2})$	$\lambda_0\left(Wm^{-1}K^{-1}\right)$
Value	$8.51514\times(10)^{10}$	$11.4508\times(10)^{10}$	$3.11\times(10)^{-5}$	3620	1000	1076	2.4

The displacements, stresses and temperature function due to a vertical dip-slip dislocation source through the point $(0,0,h)$ are computed numerically and are presented graphically.

To make the quantities dimensionless, the followings are defined

$$Y = \frac{y}{h},\ Z = \frac{z}{h},\ T = \frac{ct}{h^2},\ U_i = \frac{\pi\mu h u_i}{D_{23}},\ \sum_{ij} = \frac{\pi h^2\sigma_{ij}}{D_{23}},\ \Theta = \frac{\pi\mu h^2\alpha_t\theta}{D_{23}}. \tag{43}$$

The temperature difference function for line heat source through the point $(0,0,h)$ is computed by making it dimensionless as $\Theta = \frac{\lambda_0\theta}{q'}$. All the results mentioned in Eqs. (5) to (26b) are in Laplace transform domain. For the limiting isothermal and adiabatic cases, the results will be independent of *s* and are given in Eqs. (27) to (40). In general, inverse Laplace transform of the obtained results is to be taken. For computation of the inverse Laplace transform, Schapery's formula is used [60]. Though an extensive analysis of performance comparison of numerical inversion methods for Laplace and Hankel integral transforms in engineering problems has been done in [61], wherein better methods of Laplace inversion have been listed, but in the present case of study, the level of accuracy could also be obtained by Schapery's method. Gauss quadrature formula has been used for evaluation the semi-infinite integrals.

The variation of dimensionless displacements (U_i) with dimensionless horizontal distance (Y) at different depths Z=0, 0.5, 1.5, 5 are exhibited in Figs. 2 to 5 respectively. On the surface of half space i.e. at Z=0, the horizontal displacement decreases first and then increase and approaches to zero thereafter. Similar profile is found for Z=0.5. Below the source line (i.e. at Z=1.5, 5), the horizontal displacement increases first, reaches to their maximum and then decreases and approaches to zero. On the surface, the vertical displacement first increases, reaches up to its maximum and then decreases. The trend of the vertical displacement is similar for all Z and the

peaks of displacement decrease with the increase in the distance of the receiving point from the source. The results of displacements for the two limiting cases (adiabatic, isothermal) are also compared. These four Figs. reveal that the difference between isothermal and adiabatic cases is considerable at Y=0 for horizontal displacement and at peak points for vertical displacement.

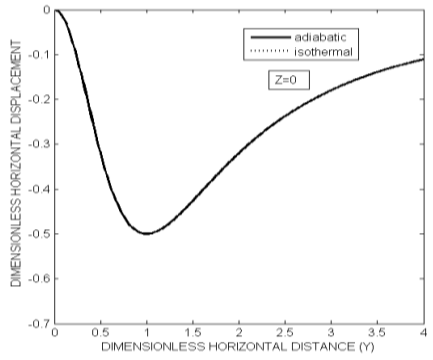

(a)

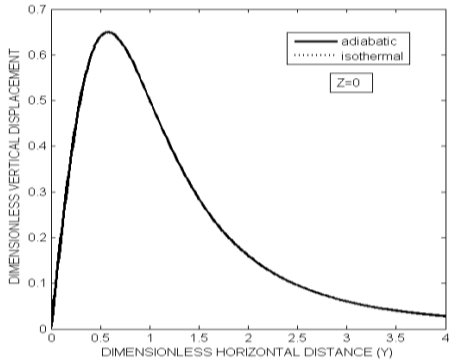

(b)

Fig.2
Variation of displacements with Y for Z=0; (a) Horizontal displacement, (b) Vertical displacement.

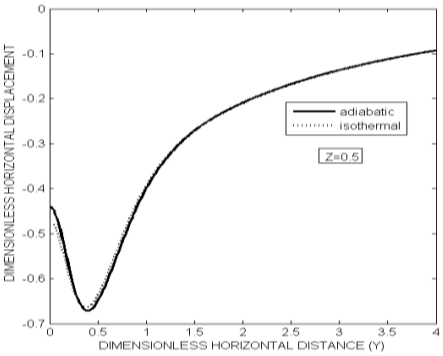

(a)

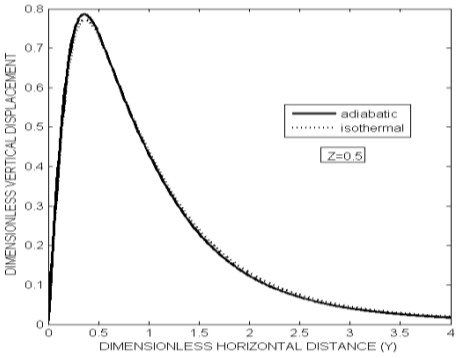

(b)

Fig.3
Variation of displacements with Y for Z=0.5; (a) Horizontal displacement, (b) Vertical displacement.

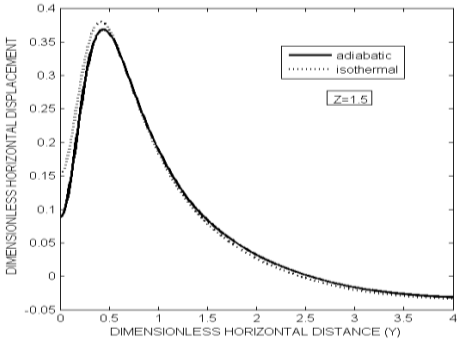

(a)

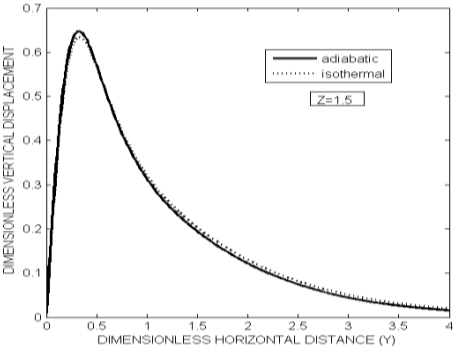

(b)

Fig.4
Variation of displacements with Y for Z=1.5; (a) Horizontal displacement, (b) Vertical displacement.

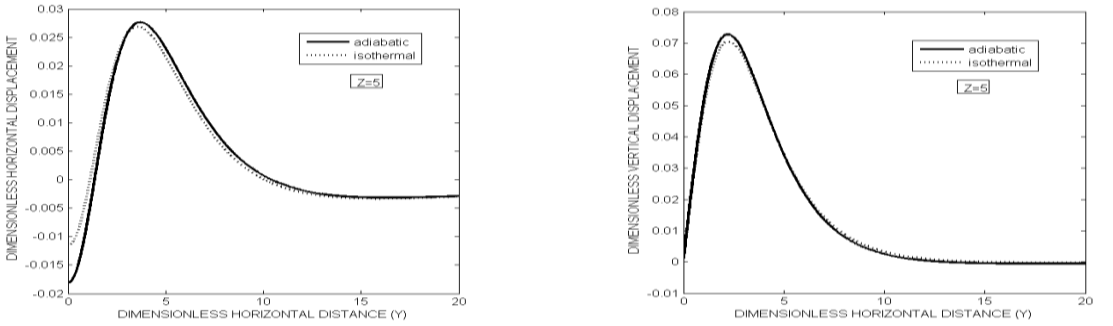

(a) (b)

Fig.5
Variation of displacements with Y for Z=5; (a) Horizontal displacement, (b) Vertical displacement.

The variations of stresses $\sum_{yy}$, $\sum_{zz}$, $\sum_{yz}$ with Y are shown in Figs. 6 to 9 for Z=0, 0.5, 1.5 and 5 respectively. $\sum_{zz}$ and $\sum_{yz}$ are zero along Y on the surface as the surface is traction free. On the surface, $\sum_{yy}$ decrease rapidly and then increases and approaches to zero. For Z=0.5, 1.5 and 5, it first go up, reaches to its maximum, then goes down up to its minimum and then approaches to zero. At Z=0.5, $\sum_{zz}$ inceases fastly upto its maxima then decreases rapidly and become stable as Y increases. Below the fault line, it first decreases rapidly, then increases smoothly and approaches to zero. The shear stress $\sum_{yz}$ decreases rapidly to its minimum and then increases smoothly for Z=0.5, 1.5 and 5. The difference of two limiting cases is found prominent on the peaks of the curves. It is also observed that maximum variation of stresses occur upto that Y which is equal to the considered Z.

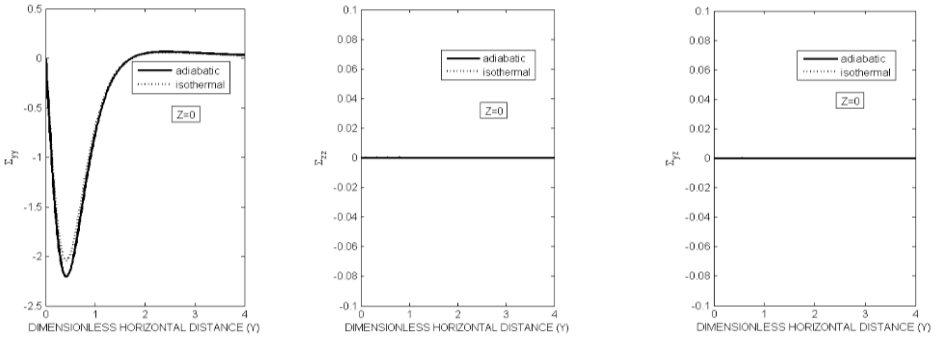

(a) (b) (c)

Fig.6
Variation of stresses with Y at Z=0 ; (a) $\sum_{yy}$, (b) $\sum_{zz}$, (c) $\sum_{yz}$.

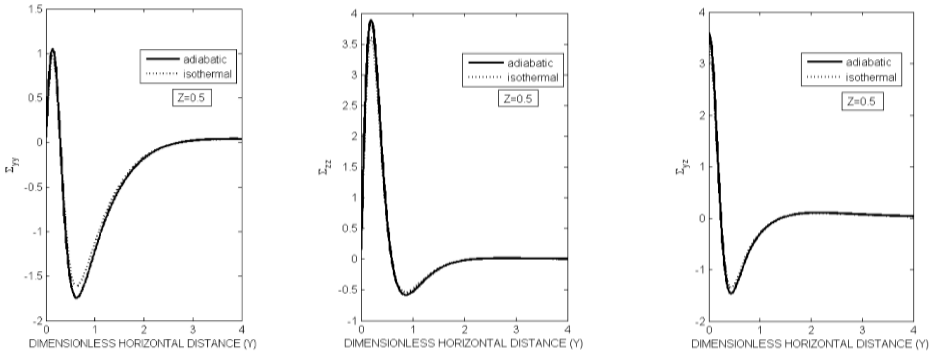

(a) (b) (c)

Fig.7
Variation of stresses with Y at Z=0.5; (a) $\sum_{yy}$, (b) $\sum_{zz}$, (c) $\sum_{yz}$.

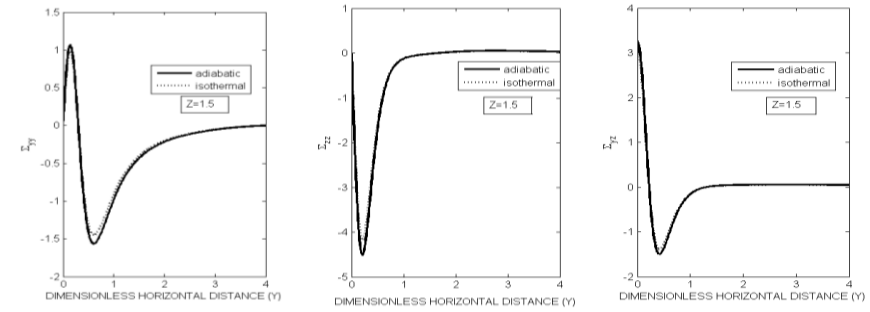

(a) (b) (c)

Fig.8
Variation of stresses with Y at Z=1.5 ; (a) $\sum_{yy}$, (b) $\sum_{zz}$, (c) $\sum_{yz}$.

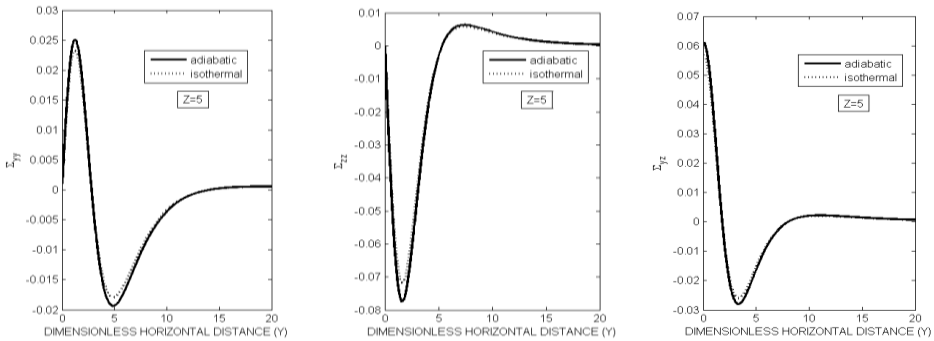

(a) (b) (c)

Fig.9
Variation of stresses with Y at Z=5; (a) $\sum_{yy}$, (b) $\sum_{zz}$, (c) $\sum_{yz}$.

The depth profile of displacements at Y=1 for the adiabatic and isothermal cases are shown in Fig. 10. Above the source, U_y is negative which implies that the tangential displacement, which is maximum in magnitude at the free surface, is in a direction opposite to y-axis. Below the source, U_y is positive and increases with depth upto Z=1.6. When the depth goes further, U_y decreases. This is also physically acceptable as far below the source, displacements are negligible. The vertical displacement is also maximum at the surface and deceases first upto the source depth. Further below the source, it increases slightly and then decreases smoothly with depth. Near the source line, the difference of the two limiting cases is considerable. The depth profile of stresses at Y=1 is exhibited in Fig. 11. The difference between two limiting cases is noticeable at peak points. At far distances, both the curves coincides and approaches to zero. It is important to note here that stress jump across the source depth is maximum for all stresses.

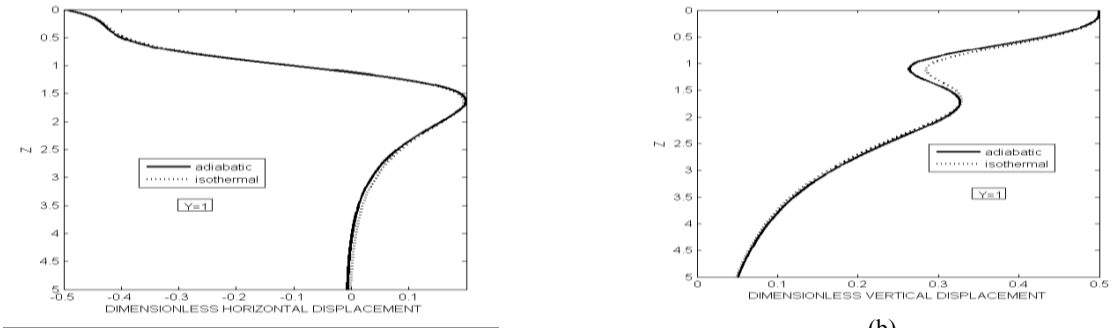

(a) (b)

Fig.10
Variaton of displacements with Z for Y=1; (a) Horizontal displacement, (b) Vertical displacement.

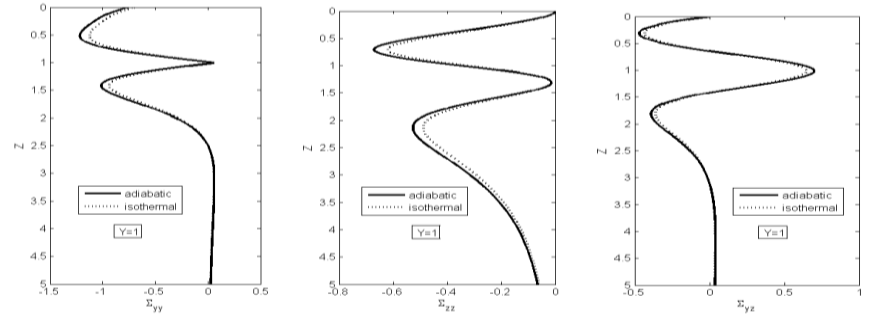

(a) (b) (c)

Fig.11
Variation of stresses with Z at Y=1 ; (a) $\sum_{yy}$, (b) $\sum_{zz}$, (c) $\sum_{yz}$.

Fig. 12 represents the variation of temperature function along the depth Z for different times T=0.0001, 1, 10 and 10000 at Y=1 and 2. Near the free surface, the temperature function decreases for Y=1. As we move vertically downwards to the source, it increases rapidly, approaches to its maximum after crossing the source line and then decreases. When T is very small (adiabatic condition), the temperature has highest amplitude. T=10000 is the case for the isothermal condition. For Y=2, temperature function increases along Z, approaches to its maximum and becomes stable with depth. The lateral variation of temperature function at different times T=0.0001, 1, 10 and 10000 for different Z=0, 1 and 5 is shown in Fig. 13. The temperature function first increases along Y, then decreases fast and become stable as Y increases. It is noticed that near the source (Z=1), temperature difference is very small in comparison to its neighborhood. All the curves for different values of T merge for large value of Y. Temperature function has highest magnitude for adiabatic conditions and is zero for isothermal condition. Figs. 12 and 13 validate the importance of consideration of thermoelastic model of the medium. It is noticed from the Figs 12 and 13 that magnitude of temperature function is very small and therefore, the contribution of the temperature change towards displacement and stresses leads to small changes in their values with change of temperature. Naeeni et al. [39] made similar observation and showed that amplitudes and arrival time of seismic waves slightly change when the thermal properties are taken into account.

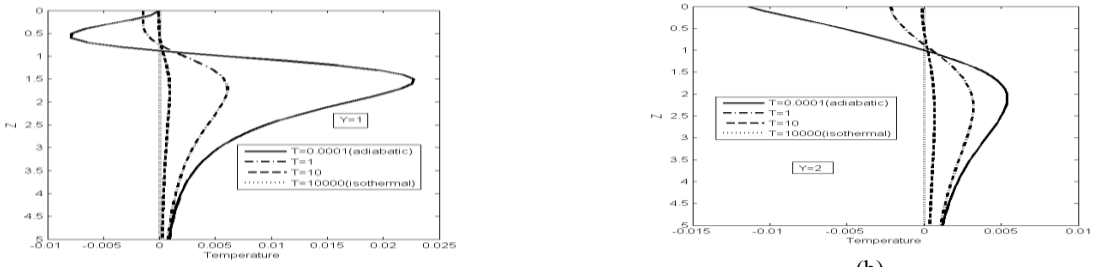

(a) (b)

Fig.12
Variation of temperature function Θ along Z for T=0.001, 1, 10 and 10000; (a) at Y=1 (b) Y=2.

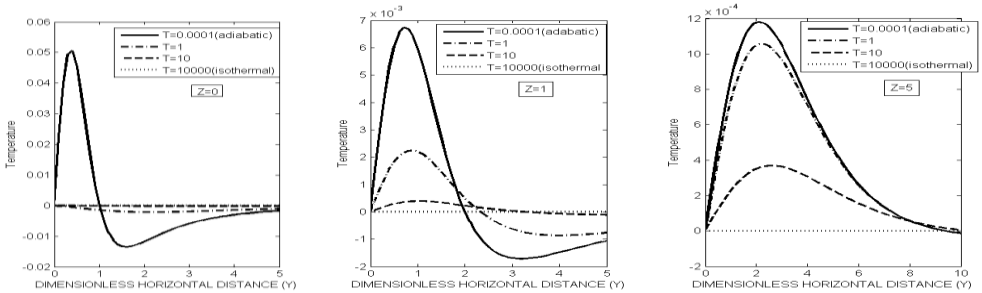

(a) (b) (c)

Fig.13
Variation of temperature function Θ along Y for T=0.001, 1, 10 and 10000; (a) at Z=0 (b) Z=1, (c) Z=5.

Time history of temperature function at different depths Z=0, 1, 2, 5 at Y=1 and 2 is presented in Fig. 14. Initially, temperature function has large variation at different depths. As the time elapses, all the curves merge. The negative temperature function is distributed near the surface of the half-space. Contour map of temperature difference function at T=1 and T=10000 for a line heat source at $(0,0,h)$ is shown in Fig. 15 for constant temperature at the surface. The gradient of temperature difference function is very large between the line heat source and the surface of half-space. This means that a large amount of heat energy is bounded within this region and the solids with a zero temperature increment surface are in a good heat resistance state. Fig 15 (b) has a good agreement with the results of static problem [35] which validate the results of the present work.

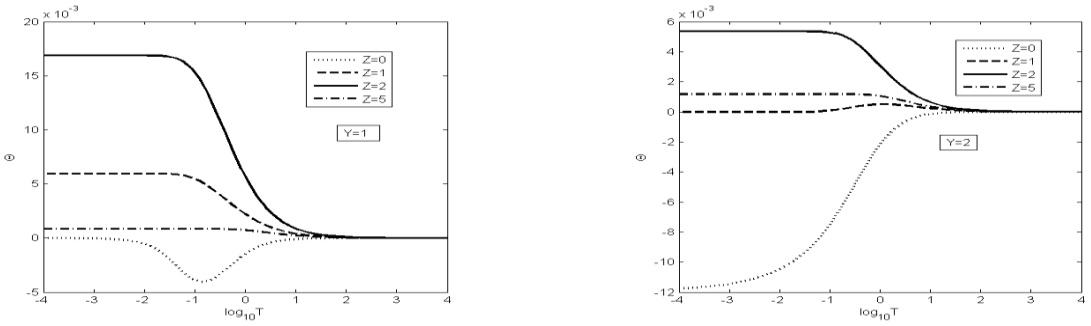

(a) (b)

Fig.14
Variation of temperature function Θ along T for Z=0, 1, 2, 5; (a) at Y=1 (b) at Y=2.

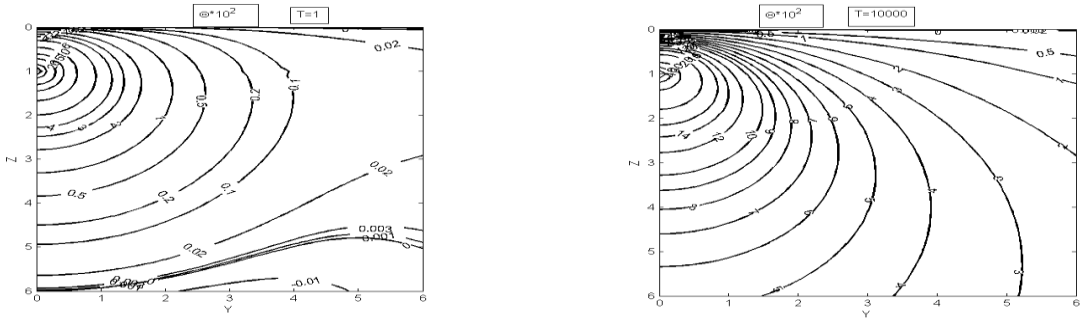

(a) (b)

Fig.15
Contour map of temperature function Θ (a) T=1 (b) T=10000.

9 CONCLUSIONS

A study of the quasi-static deformation of a homogeneous isotropic thermoelastic half-space due to two dimensional buried seismic sources has been carried out in this paper. The closed form expressions for temperature function, stresses and displacements have been obtained in the transformed domain using Airy stress function approach. The case of dip-slip dislocation source is studied in detail and the solutions are evaluated analytically for two limiting cases viz. adiabatic and isothermal. The results of the earlier studies [9] and [35] of deformation of elastic medium due to seismic sources and static problem of a line heat source respectively have been obtained as a particular case of the present study so that the results are verified. Displacements are dominant in the region near to the source and the tangential displacement changes its orientation as the level of source depth is crossed. The lateral variation of planar stresses is significant at depths near to the source. A considerable change in temperature function in the presence of seismic source but in the absence of heat source confirms the importance of thermoelastic model. Numerical results indicate that, on the surface of half-space, there is a large variation in temperature due to dip-slip dislocation inside the half-space. There is temperature fall (temperature difference is negative) just above the source but below the source, temperature increases to attains its maxima. This variation is observed for small times (at the

time of dislocation). A noticeable difference between adiabatic and isothermal cases for displacements and stresses is also observed. In the light of these critical findings, it can be concluded that a thermoelastic model is more appropriate for realistic predictions.

APPENDIX A

Eq. (4b) can be rewritten as:

$$2\mu\varepsilon_{yy} = (1-\upsilon)\,\sigma_{yy} - \upsilon\sigma_{zz} + \alpha_0\theta,\; 2\mu\varepsilon_{zz} = (1-\upsilon)\,\sigma_{zz} - \upsilon\sigma_{yy} + \alpha_0\theta,\; 2\mu\varepsilon_{yz} = \sigma_{yz} \tag{A.1}$$

where $\upsilon = \dfrac{\lambda}{2(\lambda+\mu)}$ is Poisson's ratio, $\alpha_0 = (1-2\upsilon)\beta$, $\varepsilon_{ij} = \dfrac{1}{2}\left(u_{i,j} + u_{j,i}\right)$ are components of strain tensor and satisfy the compatibility equation

$$\varepsilon_{yy,zz} + \varepsilon_{zz,yy} = 2\varepsilon_{yz,yz} \tag{A.2}$$

Eq. (2) can be written as:

$$\sigma_{yy,y} + \sigma_{yz,z} = 0,\; \sigma_{zy,y} + \sigma_{zz,z} = 0, \tag{A.3}$$

Using Eqs. (A.1), (A.3) and (4a) in (A.2) and (3), we get

$$\nabla^2(\nabla^2 U + 2\eta\theta) = 0,\; \lambda_0\nabla^2\theta - \left(\rho C_e + \frac{\alpha_0^2 T_0}{\mu(1-2\upsilon)}\right)\dot{\theta} - \frac{\alpha_0 T_0}{2\mu}(\nabla^2\dot{U}) = 0 \tag{A.4}$$

where $\eta = \alpha_0 / \left(2(1-\upsilon)\right)$.

Applying Laplace transform on (A.4), we get Eqs. (5) and (6).

REFERENCES

[1] Steketee J. A., 1958, On Volterra's dislocations in a semi-infinite elastic medium, *Canadian Journal of Physics* **36**: 192-205.

[2] Maruyama T., 1964, Statical elastic dislocations in an infinite and semi-infinite medium, *Bulletin of the Earthquake Research Institute* **42**: 289-368.

[3] Maruyama T., 1966, On two-dimensional elastic dislocations in an infinite and semi-infinite medium, *Bulletin of the Earthquake Research Institute* **44**: 811-871.

[4] Savage J.C., 1974, *Dislocations in Seismology, Dislocation Theory: A Treatise,* New York, Marcel Dekker.

[5] Savage J.C., 1980, *Dislocations in Seismology, Dislocations in Solids*, Amsterdam, North Holland.

[6] Freund L.B., Barnett D.M., 1976, A two dimensional analysis of surface deformation due to dip-slip faulting, *Bulletin of the Seismological Society of America* **66**: 667-675.

[7] Okada Y., 1985, Surface deformation due to shear and tensile faults in a half-space*, Bulletin of the Seismological Society of America* **75**(4): 1135-1154.

[8] Okada Y., 1992, Internal deformation due to shear and tensile faults in a half-space*, Bulletin of the Seismological Society of America* **82**(2): 1018-1040.

[9] Rani S., Singh S.J., Garg N.R., 1991, Displacements and stresses at any point of a uniform half space due to two-dimensional buried sources, *Physics of the Earth and Planetary Interiors* **65**: 276-282.

[10] Cohen S.C., 1992, Post seismic deformation and stresses diffusion due to visco-elasticity and comments on the modified Elsasser model, *Journal of Geophysical Research* **97**: 15395-15403.

[11] Singh S.J., Rani S., 1996, 2-D modeling of the crustal deformation associated with strike-slip and dip-slip faulting in the Earth, *Proceedings of the Indian Academy of Science* **66**: 187-215.

[12] Singh M., Singh S.J., 2000, Static deformation of a uniform half-space due to a very long tensile fault, *Journal of Earthquake Technology* **37**: 27-38.

[13] Singh S.J., Kumar A., Rani S., Singh M., 2002, Deformation of a uniform half-space due to a long inclined tensile fault, *Geophysical Journal International* **148**: 687-691.
[14] Tomar S.K., Dhiman N.K., 2003, 2-D Deformation analysis of a half-space due to a long dip-slip fault at finite depth, *Proceedings of the Indian Academy of Science* **112**(4): 587-596.
[15] Rani S., Verma R.C., 2013, Two-dimensional deformation of a uniform half-space due to non-uniform movement accompanying a long vertical tensile fracture, *Journal of Earth System Science* **122**(4): 1055-1063.
[16] Gade M., Raghukanth S.T.G., 2015, Seismic ground motion in micro polar elastic half-space, *Applied Mathematical Modelling* **39**: 7244-7265.
[17] Sahrawat R.K., Godara Y., Singh M., 2014, Static deformation of a uniform half- space with rigid boundary due to a long dip-slip fault of finite width, *International Journal of Engineering and Technical Research* **2**(5): 189-194.
[18] Volkov D., 2009, An inverse problem for faults in elastic half space, *ESAIM: Proceedings* **26**: 1-23.
[19] Volkov D., Vousin C., Ionescu I.R., 2017, Determining fault geometries from surface displacements, *Pure and Applied Geophysics* **174**(4): 1659-1678.
[20] Singh S.J., Garg N. R., 1986, On the representation of two-dimensional seismic sources, *Acta Geophysica* **34**: 1-12.
[21] Singh S.J., Rani S., 1991, Static deformation due to two dimensional seismic sources embedded in an isotropic half-space in welded contact with an orthotropic half-space, *Journal of Physics of the Earth* **39**: 599-618.
[22] Rani S., Singh S. J., 1992, Static deformation of a uniform half-space due to a long dip-slip fault, *Geophysical Journal International* **109**: 469-476.
[23] Rani S., Singh S.J., 1992, Static deformation of two welded half-spaces due to dip-slip faulting, *Proceedings of the Indian Academy of Science* **101**: 269-282.
[24] Singh S.J., Rani S., Garg N. R., 1992, Displacement and stresses in two welded half spaces caused by two-dimensional buried sources, *Physics of the Earth and Planetary Interiors* **70**: 90-101.
[25] Garg N.R., Madan D.K., Sharma R.K., 1996, Two-dimensional deformation of an orthotropic elastic medium due to seismic sources, *Physics of the Earth and Planetary Interiors* **94**(1): 43-62.
[26] Singh S. J., Punia M., Kumari G., 1997, Deformation of a layered half-space due to a very long dip-slip fault, *Proceedings of the Indian National Science Academy* **63**(3): 225-240.
[27] Rani S., Bala N., 2006, 2-D deformation of two welded half-spaces due to a blind dip-slip fault, *Journal of Earth System Science* **115**: 277-287.
[28] Rani S., Bala N., Verma R.C., 2012, Displacement field due to non-uniform slip along a long dip-slip fault in two welded half-spaces, *Journal of Earth Science* **23**(6): 864-872.
[29] Malik M., Singh M., Singh J., 2013, Static deformation of a uniform half-space with rigid boundary due to a vertical dip-slip line source, *IOSR Journal of Mathematics* **4**(6): 26-37.
[30] Debnath S. K., Sen S., 2013, Pattern of stress-strain accumulation due to a long dip slip fault movement in a viscoelastic layered model of the lithosphere –asthenosphere system, *International Journal of Applied Mechanics and Engineering* **18**(3): 653-670.
[31] Godara Y., Sahrawat R. K., Singh M., 2014, Static deformation due to two-dimensional seismic sources embedded in an isotropic half-space in smooth contact with an orthotropic half-space, *Global Journal of Mathematical Analysis* **2**(3): 169-183.
[32] Verma R.C., Rani S., Singh S. J., 2016, Deformation of a poroelastic layer overlying an elastic half-space due to dip-slip faulting, *International Journal for Numerical and Analytical Methods in Geomechanics* **40**: 391-405.
[33] Pan E., 1990, Thermoelastic deformation of a transversely isotropic and layered half-space by surface loads and internal sources, *Physics of the Earth and Planetary Interiors* **60**: 254-264.
[34] Ghosh M.K., Kanoria M., 2007, Displacements and stresses in composite multi-layered media due to varying temperature and concentrated load*, Applied Mathematics and Mechanics* **28**(6): 811-822.
[35] Hou P.F., Tong J., Xiong S.M., Hu J.F., 2012, Two-dimensional Green's functions for semi-infinite isotropic thermoelastic plane, *Zeitschrift für Angewandte Mathematik und Physik* **64**: 1587-1598.
[36] Jacquey A.B., Cacace M., Blocher G., Wenderoth M. S., 2015, Numerical investigation of thermoelastic effects on fault slip tendency during injection and production of geothermal fluids, *Energy Procedia* **76**: 311-320.
[37] Marin M., Florea O., Mahmoud S.R., 2015, A result regarding the seismic dislocations in micro stretch thermoelastic bodies, *Mathematical Problems in Engineering* **2015**: 1-8.
[38] Vashisth A.K., Rani K., Singh K., 2015, Quasi-static planar deformation in a medium composed of elastic and thermoelastic solid half spaces due to seismic sources in an elastic solid, *Acta Geophysica* **63**(3): 605-633.
[39] Naeeni M.R., Eskandari-Ghadi M., Ardalan A.A., Rahimian M., Hayati Y., 2013, Analytical solution of coupled thermoelastic axisymmetric transient waves in a transversely isotropic half-space, *Journal of Applied Mechanics* **80**(2): 024502 (1-7).
[40] Hayati Y., Eskandari-Ghadi M., Raoofian M., Rahimian M., Ardalan A.A., 2013, Dynamic Green's functions of an axisymmetric thermoelastic half-space by a method of potentials, *Journal of Engineering Mechanics* **139**(9): 1166-1177.
[41] Naeeni M.R., Eskandari-Ghadi M., Ardalan A.A., Pak R.Y.S., 2014, Asymmetric motion of a transversely isotropic thermoelastic half-space under time-harmonic buried source, *Zeitschrift für Angewandte Mathematik und Physik* **65**(5): 1031-1051.

[42] Naeeni M.R., Ghadi M.E., Ardalan A.A., Sture S., Rahimian M., 2015, Transient response of a thermoelastic half-space to mechanical and thermal buried sources, *Journal of Applied Mathematics and Mechanics* **95**(4): 354-376.

[43] Eskandari-Ghadi M., Raoofian-Naeeni M., Pak R.Y.S., Ardalan A.A., Morshedifard A., 2017, Three dimensional transient Green's functions in a thermoelastic transversely isotropic half-space, Journal *of Applied Mathematics and Mechanics* **97**: 1611-1624.

[44] Kordkheili H.M., Amiri G.G., Hosseini M., 2016, Axisymmetric analysis of a thermoelastic isotropic half-space under buried sources in displacement and temperature potentials, *Journal of Thermal Stresses* **40**: 237-254.

[45] Nowacki W., 1966, Green's functions for a thermoelastic medium (quasi-static problem), *Bulletin of Institute Political Jasi* **12**(3-4): 83-92.

[46] Cohen S.C., 1996, Convenient formulas for determining dip-slip fault parameters from geophysical observables, *Bulletin of the Seismological Society of America* **86**(5): 1642-1644.

[47] Kato N., 2001, Simulation of seismic cycles of buried intersecting reverse faults, *Journal of Geophysical Research: Solid Earth* **106**(B3): 4221-4232.

[48] Cattin R., Loevenbruck A., Pichon X.L., 2004, Why does the co-seismic slip of the 1999 Chi-Chi (Taiwan) earthquake increase progressively northwestward on the plane of rupture? *Tectonophysics* **386**: 67-80.

[49] Mitsui Y., Hirahara K., 2007, Two-dimensional model calculations of earthquake cycle on a fluid-infiltrated plate interface at a subduction zone: Focal depth dependence on pore pressure conditions, *Geophysical Research Letters* **34**(9): L09310 (1-6).

[50] Mitsui Y., Hirahara K., 2008, Long-term slow slip events are not necessarily caused by high pore fluid pressure at the plate interface: An implication from two-dimensional model calculations, *Geophysical Journal International* **174**: 331-335.

[51] Kanda R.V., Simons M., 2012, Practical implications of the geometrical sensitivity of elastic dislocation models for field geologic surveys, *Tectonophysics* **560-561**: 94-104.

[52] Zakian P., Khaji N., Soltani M., 2017, A Monte Carlo adapted finite element method for dislocation simulation of faults with uncertain geometry, *Journal of Earth System Science* **126**(7): 105(1-22).

[53] Lay T., Wallace T. C., 1995, *Modern Global Seismology,* Academic Press, New York.

[54] Banerjee P.K., 1994, *The Boundary Element Methods in Engineering*, McGraw-Hill book company, New York.

[55] Ben-Menahem A., Singh S. J., 1981, *Seismic Waves and Sources*, Springer-Verlag, New York.

[56] Barber J.R., 2004, *Elasticity*, Kluwer academic publishers, New York.

[57] Erdelyi A., 1954, Bateman *Manuscript Project-Tables of Integral Transforms*, McGraw Hill book company, New York.

[58] Ahrens T.J., 1995, *Mineral Physics and Crystallography: A Handbook of Physical Constants*, American Geophysical Union, Washington.

[59] Aki K., Richards P.G., 1980, *Quantitative Seismology: Theory and Methods*, Freeman and Company, San Francisco.

[60] Schapery R.A., 1962, Approximate methods of transform inversion for viscoelastic stress analysis, *Proceedings of the Fourth US National Congress of Applied Mechanics* **2**: 1075-1085.

[61] Naeeni M.R., Campagna R., Eskandari-Ghadi M., Ardalan A.A.,2015, Performance comparison of numerical inversion methods for Laplace and Hankel integral transforms in engineering problems, *Applied Mathematics and Computations* **250**: 759-775.